# Position Fusion for an Outdoor Mobile Robot

Michael Burke, Deon Sabatta
Mobile Intelligent Autonomous Systems
Council for Scientific and Industrial Research
Pretoria, South Africa
Email: mburke@csir.co.za

***Abstract*—Global Positioning Systems (GPS) provide an effective means of outdoor localisation. Unfortunately they are subject to a variety of errors, particularly in cluttered environments where GPS signal is not always available. Whilst GPS positional information includes measures of signal quality, these can not always be trusted, particularly just after a lost positional fix is regained. This paper presents the use of an Extended Kalman Filter to fuse GPS and odometric measurements, in order to improve vehicle positional and heading estimates. An odometric motion model is used to predict future positions, which are corrected by GPS measurements. Uncertainty in positional information from both GPS and odometry systems is modelled. The system has been implemented on Seekur, a terrestrial platform manufactured by Mobile Robots. Results of an experimental excursion of over 2 km are presented and show the efficacy of the system.**

## I. Introduction and Background

The ability of an agent to self-localise is crucial to any autonomous task where mobility is required. A good estimate of position is required prior to any meaningful interaction with the environment. Localisation refers to the process of estimating an agent's location within a known map. Various techniques have been developed to accomplish localisation and these can be loosely divided into relative and absolute localisation methods [1]. Relative localisation techniques rely on on-board sensors and systems to obtain a local estimate of position, whilst absolute localisation methods make use of landmarks or beacons to provide a global position estimate.

Common relative localisation techniques rely on inertial navigation systems (INS) which calculate agent position and heading through dead reckoning. A disadvantage to methods such as these is that they are subject to cumulative errors through drift induced by sensor noise, temperature effects, bias instability and imperfect calibration, which can lead to significant error in position estimates over time [2].

Cumulative errors can be mitigated through the use of absolute localisation systems, which provide fixed position estimates without cumulative positional uncertainty. Typical approaches to absolute localisation estimate an agent's relative position relative to known beacons or landmarks. The authors of [3] present a method of localisation based on recognition and matching of features with those in a simple environment model.

Unfortunately, in an urban outdoor context with long distances travelled, the placing of beacons or training on landmarks is no longer realistic. One set of approaches, which avoid tampering with the operational environment by identifying natural landmarks and localising therewith, have been developed in the context of the Simultaneous Localisation and Mapping (SLAM) problem, discussed in detail in [4]. The most common method of absolute outdoor localisation, however, is the use of Global Positioning Systems (GPS).


Fig. 1. Seekur, the CSIR Autonomous Rover on which the system was implemented.

GPS provides an accurate estimate of absolute position by using signals received from multiple satellites. These satellites are non-geostationary, which means that the position and number of satellites change with time and influence the system's precision [5]. GPS is subject to a variety of errors which affect its performance, such as satellite geometry, shifts in orbits, multipath, atmospheric effects, numerical calculation errors and relativistic effects. Information regarding these error sources is readily available and a variety of schemes have been developed to compensate for these errors.

Differential GPS (DGPS) is one such method and makes use of base stations transmitting the difference in positions calculated using satellite signals and their known location.

This information is then used by the platform GPS to compensate for various errors. Unfortunately, a GPS unit is unable to assist in localisation over short distances, where odometry is better suited. Hence, a strategy combining absolute position estimates with relative position estimates over short distances is required.

Fusing relative and absolute position estimates not only has the benefit of allowing localisation over short distances of travel, but also allows for position estimates in cases where the GPS position estimate is unavailable or cannot be trusted, a frequent occurrence in an outdoor urban environment, where large buildings often block satellite signals. The Extended Kalman Filter (EKF), [6], is a useful tool for fusing state measurements with predicted behaviour and is commonly used in autonomous navigation systems. The authors of [3], [5] and [7] all make use of some form of the Kalman filtering to combine GPS and relative position estimates.

This paper presents the use of an EKF to combine GPS and inertial information for the CSIR autonomous rover. A new model of GPS position and heading uncertainty, differing for the various fix types and conditions affecting GPS accuracy is presented. An odometric motion model is used to estimate the rover's relative motion and a velocity motion model to predict uncertainty in position and orientation. Results captured in a long distance experimental excursion show the efficacy of the system in an outdoor urban environment.

## II. Problem Formulation

The autonomous rover on which the position fusion system is implemented is the holonomic platform pictured in Figure 1, manufactured by Mobile Robots. In this roving application, however, the platform is controlled as if non-holonomic, to better mimic a car-like driving pattern. The platform is equipped with a simple inertial navigation system that provides forward and rotational velocity estimates together with heading and planar position.

A Hemisphere GPS heading unit, using differential corrections, provides position, altitude and heading estimates in a WGS-84 co-ordinate frame. A base station transmits correctional information to the unit, which performs calculations at 5 Hz. The GPS heading unit fuses GPS heading information with that of an on-board gyroscope, to maintain heading over short signal losses.

## III. Data Fusion

### A. Extended Kalman Filter

Data fusion is accomplished by means of the Extended Kalman Filter. The EKF consists of two stages, prediction and update. A prediction of the rover heading and position is made based on a motion model and then updated based on positional and heading information obtained from the DGPS. Given a measurement $\mathbf{z}_k$, predicted state $\hat{\mathbf{x}}_{k|k-1}$ and predicted covariance $\mathbf{P}_{k|k-1}$:

$$\hat{\mathbf{x}}_{k|k-1} = \mathbf{f}(\hat{\mathbf{x}}_{k-1|k-1}, \mathbf{u}_k)$$
$$\mathbf{P}_{k|k-1} = \mathbf{F}_k \mathbf{P}_{k-1|k-1} \mathbf{F}_k^T + \mathbf{Q}_k$$

with $\mathbf{F}_k$ a first order linearisation of the system update equations $\mathbf{f}$, and $\mathbf{Q}_k$ the process noise covariance matrix. The measurement and covariance residuals are:

$$\tilde{\mathbf{y}}_k = \mathbf{z}_k - \mathbf{h}(\hat{\mathbf{x}}_{k|k-1})$$
$$\mathbf{S}_k = \mathbf{H}_k \mathbf{P}_{k|k-1} \mathbf{H}_k^T + \mathbf{R}_k$$

with $\mathbf{H}_k$ a first order linearisation of the measurement model $\mathbf{h}$ and $\mathbf{R}_k$ the measurement noise covariance matrix. Then, the updated state and covariance estimate is given by:

$$\hat{\mathbf{x}}_{k|k} = \hat{\mathbf{x}}_{k|k-1} + \mathbf{K}_k \tilde{\mathbf{y}}_k$$
$$\mathbf{P}_{k|k} = (\mathbf{I} - \mathbf{K}_k \mathbf{H}_k) \mathbf{P}_{k|k-1}$$

Here, $\mathbf{K}_k = \mathbf{P}_{k|k-1} \mathbf{H}_k^T \mathbf{S}_k^{-1}$ is the optimal Kalman gain for a linear system.

### B. Vehicle Modelling

The state update equations for the autonomous rover are provided in (1) - (3) by the velocity motion model of [8].

$$x_k = x_{c_{k-1}} + \frac{v_{k-1}}{\omega_{k-1}} \sin(\theta_{k-1} + \omega_{k-1}\Delta t) \tag{1}$$
$$y_k = y_{c_{k-1}} - \frac{v_{k-1}}{\omega_{k-1}} \cos(\theta_{k-1} + \omega_{k-1}\Delta t) \tag{2}$$
$$\theta_k = \theta_{k-1} + \omega_{k-1}\Delta t \tag{3}$$

where

$$x_{c_k} = x_k - \frac{v_k}{\omega_k} \sin\theta_k$$
$$y_{c_k} = y_k + \frac{v_k}{\omega_k} \cos\theta_k$$

is the centre of rotation of the platform, $v_k$ and $\omega_k$ the forward and rotational velocities at sample $k$ respectively, and $x_k, y_k$ the right handed planar co-ordinates with $y_k$ facing the front of the platform. Assuming the velocity inputs are subject to zero-mean Gaussian noise and the presence of an additional noise variable acting on the rover orientation, Equations (1) - (3) lead to (4) - (6).

$$x_k = x_{k-1} - \frac{v_{k-1} + \epsilon_v}{\omega_{k-1} + \epsilon_\omega}(\sin\theta_{k-1} - \sin(\theta_{k-1} + (\omega_{k-1} + \epsilon_\omega)\Delta t) \tag{4}$$
$$y_k = y_{k-1} + \frac{v_{k-1} + \epsilon_v}{\omega_{k-1} + \epsilon_\omega}(\cos\theta_{k-1} - \cos(\theta_{k-1} + (\omega_{k-1} + \epsilon_\omega)\Delta t)) \tag{5}$$
$$\theta_k = \theta_{k-1} + (\omega_{k-1} + \epsilon_\omega)\Delta t + \epsilon_\gamma \Delta t \tag{6}$$

Here, $\epsilon_v$, $\epsilon_\omega$ and $\epsilon_\gamma$ are zero-mean, normal random variables with covariances $\sigma_v^2$, $\sigma_\omega^2$ and $\sigma_\gamma^2$ respectively. Linearising these

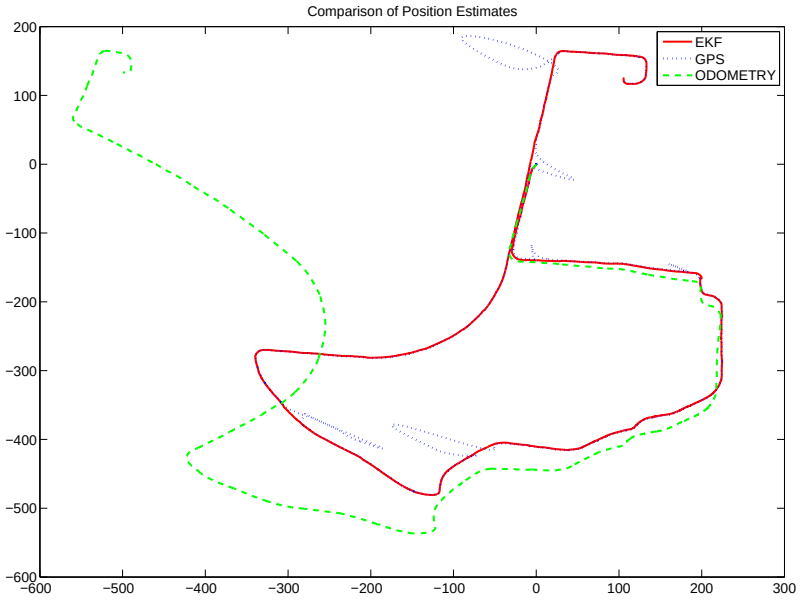


Fig. 2. Raw odometry compared to GPS and fused position.

equations using Taylor expansion gives

$$x_k = x_{k-1} - \frac{v_{k-1}}{\omega_{k-1}}(\sin\theta_{k-1} - \sin(\theta_{k-1} + \omega_{k-1}\Delta t)) + (\theta_{k-1} - \delta)\frac{\partial x_k}{\partial \theta_{k-1}} + \epsilon_v \frac{\partial x_k}{\partial \epsilon_v} + \epsilon_\omega \frac{\partial x_k}{\partial \epsilon_\omega} \quad (7)$$

$$y_k = y_{k-1} + \frac{v_{k-1}}{\omega_{k-1}}(\cos\theta_{k-1} - \cos(\theta_{k-1} + \omega_{k-1}\Delta t)) + (\theta_{k-1} - \delta)\frac{\partial y_k}{\partial \theta_{k-1}} + \epsilon_v \frac{\partial y_k}{\partial \epsilon_v} + \epsilon_\omega \frac{\partial y_k}{\partial \epsilon_\omega} \quad (8)$$

$$\theta_k = \theta_{k-1} + \omega_{k-1}\Delta t + \epsilon_\omega \Delta t + \epsilon_\gamma \Delta t \quad (9)$$

where $\delta$ is the angle about which the equations are linearised.

Equations (7)-(9) have the desirable property of separate system and noise terms. Hence, setting the random noise variables to zero provides the state update equations. This property also allows the system covariance update to be calculated as the sum of the system covariance and the noise covariance passed through the system model.

Given a linear system $\mathbf{Y} = \mathbf{TX}$, the transform of the mean and covariance of Gaussian random variables passed through is given by $\mathbf{E}[\mathbf{Y}] = \mathbf{TE}[\mathbf{X}]$ and $\mathbf{Cov}[\mathbf{Y}] = \mathbf{TCov}[\mathbf{X}]\mathbf{T}^T$ respectively. Therefore, the system covariance update equation is $\mathbf{C} = \mathbf{T}_u\mathbf{C}_u\mathbf{T}_u^T + \mathbf{T}_x\mathbf{C}_x\mathbf{T}_x^T$ Here, subscript $x$ represents system contributions and subscript $u$, noise contributions. It can now be easily shown that

$$\mathbf{T}_u = \begin{bmatrix} \frac{\partial x_k}{\partial \epsilon_v} & \frac{\partial x_k}{\partial \epsilon_\omega} & 0 \\ \frac{\partial y_k}{\partial \epsilon_v} & \frac{\partial y_k}{\partial \epsilon_\omega} & 0 \\ 0 & \Delta t & \Delta t \end{bmatrix}_{\epsilon_v = \epsilon_\omega = \epsilon_\phi = 0}$$

$$\mathbf{C}_u = \begin{bmatrix} \sigma_v^2 & 0 & 0 \\ 0 & \sigma_\omega^2 & 0 \\ 0 & 0 & \sigma_\phi^2 \end{bmatrix}$$

where

$$\frac{\partial x_k}{\partial \epsilon_v} = -\frac{1}{\omega_k}(\sin\theta_k - \sin(\theta_k + \omega_k\Delta t))$$
$$\frac{\partial x_k}{\partial \epsilon_\omega} = \frac{v_k}{\omega_k}(-\frac{\partial x_k}{\partial \epsilon_v} + \Delta t\cos(\theta_k + \omega_k\Delta t))$$
$$\frac{\partial y_k}{\partial \epsilon_v} = \frac{1}{\omega_k}(\cos\theta_k - \cos(\theta_k + \omega_k\Delta t))$$
$$\frac{\partial y_k}{\partial \epsilon_\omega} = \frac{v_k}{\omega_k}(-\frac{\partial y_k}{\partial \epsilon_v} + \Delta t\sin(\theta_k + \omega_k\Delta t))$$

Unfortunately, this system is not valid for $\omega_k = 0$. In this case the state update equations become

$$x_k = x_{k-1} + v_{k-1}\Delta t\cos\theta_{k-1}$$
$$y_k = y_{k-1} + v_{k-1}\Delta t\sin\theta_{k-1}$$
$$\theta_k = \theta_{k-1}$$

and

$$\mathbf{T}_u = \begin{bmatrix} \frac{\partial x_k}{\partial \epsilon_v} & 0 & 0 \\ \frac{\partial y_k}{\partial \epsilon_v} & 0 & 0 \\ 0 & 0 & \Delta t \end{bmatrix}$$

with

$$\frac{\partial x_k}{\partial \epsilon_v} = \Delta t \cos\theta_k$$
$$\frac{\partial y_k}{\partial \epsilon_v} = \Delta t \sin\theta_k$$

In all cases the process noise covariance is calculated as $\mathbf{Q}_k = \mathbf{T}_u \mathbf{C}_u \mathbf{T}_u^T$.

The error in autonomous rover velocity is assumed to be in the region of $5\%$, based on odometry estimates provided by the manufacturer, therefore the forward velocity standard deviation was chosen as $\sigma_v = 0.05$. A $60^\circ/hour$ drift in heading resulting from the platform INS is distributed equally between the rotational velocity and heading noise covariances, $\sigma_\omega^2$ and $\sigma_\phi^2$ respectively, unless there is no rotational motion, in which case the error is assigned wholly to the heading noise covariance, $\sigma_\phi^2$. This is due to the fact that the platform drifts in heading even when no rotational motion is exhibited, since the INS continually amplifies low frequency sensor errors due to the integrative nature of its calculations.

The state update equations from the velocity motion model could be used in the EKF, but a better system update is obtained through the odometry motion model of [8], since measurements of internal platform odometry are typically more accurate than those of velocity due to the wheel geometry of the platform. Velocities are calculated as the derivative of position measurements (taken directly from wheel encoders on the platform), which introduces an additional noise source and a loss of accuracy. The odometry motion model shows that motion between a pair of positions can be decomposed into three stages, a rotation $\delta_{rot1}$, followed by translation $\delta_{trans}$ and another rotation $\delta_{rot2}$. Given motion in these stages, the system update becomes

$$x_k = x_{k-1} + \delta_{trans}\cos(\theta_{k-1} + \delta_{rot1})$$
$$y_k = y_{k-1} + \delta_{trans}\sin(\theta_{k-1} + \delta_{rot1})$$
$$\theta_k = \theta_{k-1} + \delta_{rot1} + \delta_{rot2}$$

The three stage motion is calculated from adjacent odometry measurements as follows

$$\delta_{rot1} = \arctan 2(y_k - y_{k-1}, x_k - x_{k-1}) - \theta_k$$
$$\delta_{trans} = \sqrt{(y_k - y_{k-1})^2 + (x_k - x_{k-1})^2}$$
$$\delta_{rot2} = \theta_k - \theta_{k-1} - \delta_{rot1}$$

### C. GPS Modelling

The DGPS and heading unit used exhibits accuracies that vary based on signal quality, so various noise covariances were selected for each of the states encountered. The DGPS horizontal accuracy in positional fix, $\sigma_p$, degrades from $0.6$ m under fix type 2 (a GPS fix with differential correction) to $2.5$ m under fix type 1 (a GPS fix without differential correction). If no fix is obtained, no trust is placed in the horizontal accuracy and the corresponding covariance $\sigma_p$ is made large.

The heading unit exhibits a heading accuracy of $\sigma_\theta = 0.3^\circ$, which degrades to $\sigma_\theta = 1^\circ$ for up to 3 minutes after a GPS fix is lost. Thereafter, little trust can be placed in the heading unit's reading and $\sigma_\theta$ is made large. In the period just after signal is lost and then regained, a period of uncertainty exists, where GPS signal and fix quality appear good, but position is incorrect. This is most likely due to the least squares method used to calculate position from satellite signals. When good data returns, it takes some time for the calculation to leave a bad positional fix and converge to a least squares solution. As a result, uncertainty in position ($\sigma_p$) remains large for a short time after a fix is regained to compensate for this. The measurement noise covariance is given by (10).

$$\mathbf{R_k} = \begin{bmatrix} \sigma_p^2 & 0 & 0 \\ 0 & \sigma_p^2 & 0 \\ 0 & 0 & \sigma_\theta^2 \end{bmatrix} \tag{10}$$

Fusion calculations are performed in an East, North, Up co-ordinate frame to simplify calculations.

## IV. Experimental Results

Figure 2 shows the path followed by the autonomous rover. Odometry is plotted in green as a dashed line, GPS measurements in dotted blue and the fused data in red. Initially, the rover moved south with a GPS fix type 1. Here, more trust is placed in odometry as there is greater uncertainty in GPS position. Once the fix type improved there was less uncertainty in position estimates. Completely incorrect GPS data obtained when the fix was lost and for a short time thereafter is visible at various stages along the path.

Figure 3 shows the data obtained for the heading, East and North co-ordinates. The fused data closely follows that of the GPS, since it is typically more accurate than odometry, but corrects data well when the GPS position is not trustworthy. Odometry is quite accurate until about the nine thousandth sample, where increased errors are visible. This loss of accuracy corresponds to an incline in the road on which the robot was travelling, which introduces additional heading errors since the platform's internal heading calculations assume a planar surface. A small heading error corresponds to a larger error in position, as indicated by the East and North odometry traces.

It is difficult to determine the accuracy of the fused signal, as no ground truth is available. Figure 4 shows a plot of the path in Google Earth, which can be used as a rough estimate of the horizontal accuracy, based on its position relative to roads. Unfortunately, this is not a true measure of accuracy as there is uncertainty in the registration of images in Google Earth, but it does show that the system is accurate enough to follow a path planned using Google Earth.

## V. Conclusion

GPS data is a valuable source of absolute positional information in an outdoor autonomous application, but errors

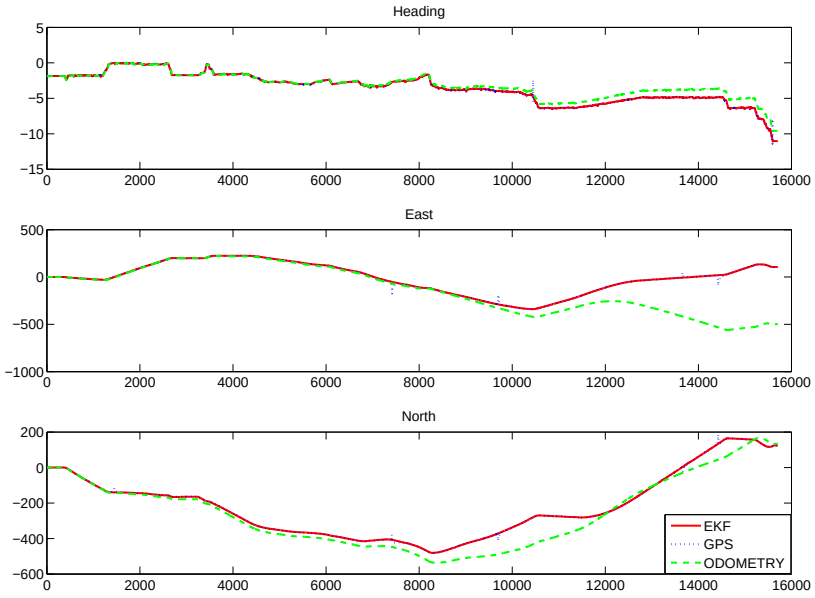


Fig. 3. Comparison of individual variables for raw odometry, GPS and fused position.


Fig. 4. Path followed overlaid in Google Earth

frequently occur in urban environments. Odometry, whilst a feasible position estimate in short distance travel, is subject to cumulative errors that increase positional uncertainty over time. Fusing relative and absolute position estimates reduces the effect of these errors and provides more certainty in positional information.

A model of the positional uncertainty of the Seekur autonomous rover platform in a non-holonomic drive configuration has been presented. The model combines velocity and odometric information for greater accuracy, but could be improved if accelerometer tilt information was available as currently a planar surface assumption is made.

Extremely good results were obtained regardless of the planar surface assumption. A path of over 2 km was traversed, and fused positional information accurate enough for autonomous driving, when used in conjunction with a suitable path planner, was obtained.

## REFERENCES

[1] P. Goel, S. Roumeliotis, and G. Sukhatme, "Robust localization using relative and absolute position estimates," in *Intelligent Robots and Systems, 1999. IROS '99. Proceedings. 1999 IEEE/RSJ International Conference on*, vol. 2, 1999, pp. 1134–1140 vol.2.

[2] O. J. Woodman, "An introduction to inertial navigation," University of Cambridge, Tech. Rep. 696, August 2007.

[3] A. Georgiev and P. Allen, "Localization methods for a mobile robot in urban environments," *Robotics, IEEE Transactions on*, vol. 20, no. 5, pp. 851–864, Oct. 2004.

[4] S. Thrun, "Robotic mapping: a survey," in *Exploring artificial intelligence in the new millennium*, G. Lakemeyer and B. Nebel, Eds. San Francisco, CA, USA: Morgan Kaufmann Publishers Inc., 2003, pp. 1–35.

[5] S. Panzieri, F. Pascucci, and G. Ulivi, "An outdoor navigation system using GPS and inertial platform," in *Advanced Intelligent Mechatronics, 2001. Proceedings. 2001 IEEE/ASME International Conference on*, vol. 2, 2001, pp. 1346–1351 vol.2.

[6] G. Welch and G. Bishop, "An introduction to the Kalman filter," Chapel Hill, NC, USA, Tech. Rep., 1995.

[7] R. Thrapp, C. Westbrook, and D. Subramanian, "Robust localization algorithms for an autonomous campus tour guide," in *Robotics and Automation, 2001. Proceedings 2001 ICRA. IEEE International Conference on*, vol. 2, 2001, pp. 2065–2071 vol.2.

[8] S. Thrun, W. Burgard, and D. Fox, *Probabilistic Robotics (Intelligent Robotics and Autonomous Agents)*. The MIT Press, 2005.